Macaranga peltata Leaf Extract Mediated Green Synthesis of Iron Nanoparticles and Their Application in Organic Dye Removal

Dissanayake D.M.K.N.[a], Perera M.A.D.[a], Karunaratne M.S.A.[a], Pahalagedara M.N.[b]
[a] Department of Materials Engineering, Faculty of Engineering, Sri Lanka Institute of Information Technology, Malabe 10115, Sri Lanka.
[b] Department of Basic Sciences, Faculty of Allied Health Sciences, University of Sri Jayewardenepura, Nugegoda 10250, Sri Lanka
kasuni0620@gmail.com, ann000461@gmail.com, mudith.k@sliit.lk, madhavinp@sjp.ac.lk

ABSTRACT

This study presents an eco-friendly method for synthesizing iron nanoparticles (FeNPs) using *Macaranga peltata* leaf extract, and evaluate their potential for degrading the organic dye methyl orange (MO). The synthesis exploits phytochemicals in the leaf extract as natural reducing and stabilizing agents. The synthesized FeNPs were characterized using UV-Vis spectroscopy, FTIR, XRD, and SEM, confirming amorphous structure and particle sizes ranging from 34–94 nm. Catalytic activity was evaluated via MO degradation experiments, achieving 85.16% efficiency within 200 minutes. The study demonstrates a sustainable wastewater treatment solution using green nanotechnology.

KEYWORDS: *Green synthesis, Iron nanoparticles, Macaranga peltata, Methyl Orange, Dye degradation, Wastewater treatment.*

1 INTRODUCTION

Nanotechnology has revolutionized many fields, including medicine, electronics, and environmental science by introducing advanced material properties at the nanoscale (ElHelaly, 2013; Yusuf, 2019). Among the broad applications of nanotechnology, the treatment of environmental pollutants is one of the most promising areas in which nanoparticles have already demonstrated their outstanding ability to degrade contaminants (Ashraf et al., 2018).

Nanoparticle synthesis methods can be divided into three main approaches: physical, chemical, and biological. However, most of the conventional synthesis methods such as chemical and physical methods involve the use of toxic chemicals and energy-intensive processes, raising concerns about their overall environmental impact (Jiang et al., 2022). In recent years, green synthesis has emerged as a sustainable, environmentally friendly alternative to produce nanoparticles. This method employs biological entities, like plant extracts, bacteria, or fungi, for nanoparticle synthesis, thereby negating the use of toxic chemicals. Among these, plant extracts have gained a lot of interest due to the abundance of bioactive compounds present in them such as ketones, aldehydes, polyphenols, caffeine, isoverbascosides and carbohydrates, serving as natural reducing and stabilizing agents to convert the metal ions into nanoparticles in the synthesis process, simplicity in preparation, and cost-effectiveness (Ebrahiminezhad et al., 2018).

1.1 Plant-Mediated Green Synthesis of Nanoparticles

There are significant studies that impress various plants involved in the process, the sizes of the nanoparticles synthesized, and their applications. A prominent example of plant-mediated synthesis involves *Cupressus sempervirens* to produce zero valent iron nanoparticles. Ebrahiminezhad et al. (2018) reported the formation nanoclusters with diameters from 9 to 31 nm, synthesized using Mediterranean cypress *(Cupressus sempervirens)* leaf branches. The reaction between the iron solution and the leaf extract was observed by noticeable color change indicating the high reduction potential of phytochemicals in this plant extract. This study highlighted iron nanoparticles' potential for removing

https://doi.org/10.54389/GPPL8880

dyes from aqueous environments. The bark extract of *Pinus eldarica* has also been used in the green synthesis of silver nanoparticles, as reported by Iravani and Zolfaghari (2013).

This study underscored *Pinus eldarica* bark extract contains polyphenolic compounds characterized by hydroxyl and carboxyl groups making it an excellent candidate for nanoparticle synthesis. It has been revealed that the exposure of *Pinus eldarica* bark extract to Ag+ ions resulted in a color change in the reaction mixture from yellowish brown to dark brown, indicating the successful formation of silver nanoparticles. In this study, the effect of pH on nanoparticle size and morphology of was highlighted, and it was shown that at lower pH values, larger nanoparticles were synthesized. In another study, Ahmed and Mustafa (2019) published a wide-ranging studies on the synthesis of gold and silver nanoparticles using lemongrass *(Cymbopogon flexuosus)* and green tea *(Camellia sinensis)*. The study identified various phyto-constituents in these plants including tannins, terpenoids, flavonoids, ketones, aldehydes, amides, and carboxylic acids which are responsible for reducing of silver ions. Among these, tannins were found to play a crucial role in both the reduction and capping of silver nanoparticles.

1.2 Overview of Macaranga peltata

Macaranga peltata belongs to the family Euphorbiaceae, is one of the common pioneer arboreal species mainly distributed in Southeast Asia, particularly in India and Sri Lanka. This species is more popularly known as "kenda" in Sri Lankan and "chandada" in India. It may reach up to 10 meters in height exhibiting a resinous tree structure with its young parts covered with velvety hairs. Its leaves are alternately arranged, measuring between 20 and 50 centimeters in length and 12 and 21 centimeters in width, characterized by a broad ovate shape and a distinct palmately 9-nerved pattern. The flowering period occurs in January to February, with yellow-green flowers clustered in long panicles in the leaf axils, and the fruit is a spherical capsule that carries a single black seed (Megha M et al., 2024).

Figure 1. *Macaranga peltata* leaf

A review of the phytochemical profile of *Macaranga peltata* shows that it is rich in secondary metabolites such as flavonoids, stilbenes, tannins, and terpenes, isolated from leaves. Preliminary phytochemical screenings has revealed the presence of some bioactive compounds including carbohydrates, alkaloids, phenolic compounds, tannins, saponins, and steroids in the plant's ethanolic extracts (Megha M et al., 2024). These bioactive compounds have been attributed to several pharmacological activities including antimicrobial, antioxidant, anti-inflammatory, anticancer, antifungal action, and other properties such as wound healing and hepatoprotection (Megha M et al., 2024). The potential therapeutic applications of these bioactive compounds underscore the importance of *Macaranga peltata* in traditional medicine and its prospective application in modern therapeutic practice (Megha M et al., 2024). In addition, recent studies have explored the potential of Macaranga peltata extracts for the green synthesis of nanoparticles, capitalizing on its bioactive compounds.

1.3 Overview of Iron Nanoparticles (FeNPs)

Over the last few years, significant attention has been paid to iron nanoparticles (FeNPs) due to their unique properties and broad potential for applications in biomedicine, environmental remediation, and catalysis. There are different synthesis methods for FeNPs including chemical reduction, various physical methods, and green synthesis using plant extracts. Among the outstanding methods for synthesizing iron nanoparticles is chemical reduction, in which iron ions (Fe^{3+}) are reduced to zero-valent iron (Fe^{0}) using reducing agents such as sodium borohydride ($NaBH_4$). This method has demonstrated that the synthesized nanoparticles are around 100 nm in size, as indicated by the black colour observed during synthesis, a characteristic of iron nanoparticles (Abdeen et al., 2013).

However, green synthesis methods have emerged as an environmentally friendly alternative for producing iron nanoparticles. This method uses natural extracts derived from plants, rich in various phytochemicals that reduce iron ions to form nanoparticles and stabilize them. For example, green synthesis using *Cupressus sempervirens* produces zero valent iron nanoparticles. Ebrahiminezhad et al. (2018) reported the formation nanoclusters with diameters from 9 to 31 nm, synthesized using Mediterranean cypress *(Cupressus sempervirens)* leaf branches. The reaction between the iron solution and the leaf extract was observed by noticeable color change indicating the high reduction potential of phytochemicals in this plant extract. This study highlighted the potential of iron nanoparticles' removing dyes from aqueous environments. In another study, it was found that green tea leaf extract (GT-Fe NPs) which contains polyphenols, acts as reducing and capping agent, mediated the synthesis of iron nanoparticles within the size range of 40-60 nm. Fe NPs were identified by the formation of strong black precipitate during the synthesis process. The synthesized particles showed very good removability and therefore, have potential application in the field of environmental remediation (Shahwan et al., 2011).

1.4 Properties of Iron Nanoparticles Relevant to Dye Degradation

Some physiochemical properties of iron nanoparticles (Fe NPs) were identified by Wanakai et al. (2019). These nanoparticles' properties have enabled them to act efficiently as catalysts in the degradation of dyes and especially methylene blue. That study discussed green synthesis, high surface area, oxidation states, fenton and fenton-like mechanisms and catalytic efficiency. The iron nanoparticles were synthesized using aqueous leaf extracts from the plants such as *Galinsoga parviflora, Conyza bonariensis* and *Bidens pilosa*, as reported by Wanakai et al. (2019). This method is ecofriendly and yields non-toxic, stable nanoparticles, which are quite essential for degradations of dyes. Also, the study emphasized the high surface area.

Due to the high surface area-to-volume ratio and their role as catalysts, iron nanoparticles are interact with dye molecules more effectively thereby enhancing their degradation. The oxidation states noted in the study also fall under the properties of iron nanoparticles relevant to dye degradation. It was emphasized that Iron is one of the versatile in mechanical engineering, and that it exists in more valencies/oxidation states. Those are ferrous and ferric. This characteristic is rather important since it determines the degree of effectiveness of the nanoparticles in catalysing the reactions, particularly in the degradation process using hydrogen peroxide. Furthermore, Wanakai et al. (2019) reported that the fenton and fenton-like mechanisms are among the properties . The study mentioned that methylene blue degradation occurs via Fenton and Fenton-like reactions. Fenton reaction is the reaction between Fe ions and H_2O_2 and yields hydroxyl radical (-OH). These radicals are highly reactive and therefore play an important role in cleaving of the dye molecules (Wanakai et al., 2019).

1.5 Application of Fe NPs in Organic Dye Removal

To address the challenge of dye contamination, various remediation strategies have been contrived. Notably, among all the remediation methods, the incorporation of nanomaterials has emerged as a promising approach. Nanomaterials have a large surface area-to-volume ratio and unique chemical properties that make them highly effective for adsorbing and degrading dye molecules in wastewater

(Ruan et al., 2018a). For example, it has been demonstrated that nano iron particles promote the decolorization of mono azo dyes via advanced oxidation processes that produce reactive species that degrade dye structures (Raman & Kanmani, 2018). The green synthesis of iron nanoparticles (Fe NPs) has received significant attention , owing to their environmentally friendly nature and potential for application in wastewater treatment, especially in dye removal. Several plant extracts have been used in the biosynthesis of Fe NPs, which then effectively show the degradation of various dyes including Methylene Blue (MB), Methyl Orange (MO), and Malachite Green (MG). This synthesis route provides not only a green alternative to chemical methods but also enables fine-tuning of the catalytic properties of the nanoparticles making them suitable for various environmental remediation applications.

Giun Tan et al. (2018) investigated the preparation of iron oxide nanoparticles using plantain peel extracts and found the particles to be very effective in the removal of both Methylene Blue and Methyl Orange dyes. The study focused on the catalytic and magnetic properties of green synthesized iron oxide nanoparticles (G-FeONPs) which showed efficacy in wastewater treatment. The reported degradation efficiencies for Methylene Blue and Methyl Orange are quite high, indicating that G-FeONPs have the potential for practical applications. In a similar vein, Ebrahiminezhad et al. (2018) have studied the green synthesis of iron nanoparticles using *Cupressus sempervirens* yielding iron nanoclusters with a mean diameter of 19 nm. Their work focused on optimization conditions for the removal of Methyl Orange and their results showed that the green synthesized iron nanoclusters showed a 95% decolorization efficiency in 6 h time. The results showed the nanoparticles effectively degraded Methyl Orange, and therefore, the potential for practical applications in dye removal during wastewater treatment applications.

Shahwan et al. (2011) extended their knowledge on Fe NPs produced from green tea leaf extract, demonstrating their role in Fenton-like catalysts in the degradation of dyes. This study has shown a rapid degradation of Methylene Blue and Methyl Orange, in which kinetic analysis indicating that Methylene Blue degradation followed a second-order reaction, In contrast, Methyl Orange degradation followed a first-order reaction . In another study, Khoirotin et al. (2023) investigated the green synthesis of Fe_3O_4 nanoparticles using green betel *(Piper betle L.)* leaf extract, demonstrating ferromagnetic properties and efficient adsorption. This study identified the highest adsorption capacity of Fe_3O_4 for methylene blue at a contact time 120 minutes with 98.75% MB degradation.

Most previous studies have focused on different metal nanoparticles synthesized using different plant extracts and their applications in environmental remediation, especially in the removal of dyes. Although the application of green-synthesized nanoparticles for organic dye removal has been widely reported, the specific role of iron nanoparticles synthesized through *Macaranga peltata* leaf extract has remained underexplored. The existing gap in the literature provides an opportunity to investigate the effectiveness and possible mechanisms by which iron nanoparticles, derived from this plant extract, may enhance the removal of organic dyes, thereby addressing environmental pollution and meeting the demand for sustainable materials in nanotechnology.

2 METHODOLOGY

2.1 Preparation of *Macaranga peltata* leaf extraction

As an initial step, the leaves of *Macaranga peltata* were collected and washed multiple times to remove any dirt and other impurities. Then, 10 g of *Macaranga peltata* leaves were measured using an analytical balance. After that, the leaves were cut into small pieces and ground with a motor and pestle and mixed with 50ml of distilled water. Next, the sample was stirred at 80 ºC temperature for 30 minutes to extract bioactive compounds efficiently. After 30 minutes, the flask was removed from the hot plate and left for a few minutes until it reached room temperature. Finally, the resultant extract was filtered using Whatman filter papers to remove leaf debris.

2.2 Green Synthesis of Iron Nanoparticles

Green synthesis was done using *Macaranga peltata* leaves extract by adding 10ml *Macaranga peltata* leaf extract to 5ml of 0.1 M ferric chloride solution in 2:1 (v/v) ratio in a conical flask. Then, the solution containing ferric chloride was stirred with a mechanical stirrer for 3 hours while the leaf extract was added dropwise . At this time, there was an immediate color change after adding the leaf extract to the iron chloride solution. A color change from pale brown to blackish brown was observed indicating the formation of iron nanoparticles (Fe NPs). Then, the solution undisturbed at room temperature for 24 hours to allow the nanoparticles to settle at the bottom of the beaker. After 24 hours, synthesized nanoparticles were separated by centrifugation at 5000 rpm for 15 minutes. Then the separated nanoparticle sample was washed twice with water and once with ethanol. Finally, the synthesized nanoparticle sample was dried at room temperature and stored in a sealed container for subsequent analysis.

2.3 Kinetic Experiment of the Degradation of Methyl Orange Dye

First, the calibration curve for methyl orange dye was prepared. Then, a 50 mg/L solution of methyl orange was prepared as a model organic dye. 2 mL of dye solution was withdrawn from the 50 mg/L dye solution and diluted it up to 10 mL by adding water into a 10 mL volumetric flask. This solution was transferred to a sample vial to record initial UV-Vis data at t=0. 50 mg of FeNPs were added to 45 mL of 50 mg/L dye solution, along with 5 mL of 10% H_2O_2. The mixture was stirred on a magnetic stirrer at room temperature to ensure proper mixing. 2mL samples were withdrawn from the mixture at time intervals of 20, 40, 60, 80, 100, 120, 140, 160, 180, 200 minutes and the absorbance was recorded at 464 nm (characteristic wavelength for methyl orange) using UV-Vis spectrophotometer. The same procedure was followed without adding Fe NPs, serving as a control experiment to investigate the degradation efficiency of Fe NPs.

The dye degradation efficiency was calculated using the following equation.

$$Degradation\ Efficiency\ (\%) = \frac{C_i - C_f}{C_i} \times 100\%$$

In this equation, C_i denotes initial concentration of dye solution, and C_f denotes concentration of dye solution after time t.

2.4 Characterization of Synthesized Nanoparticles

1. Ultraviolet-Visible (UV-Vis) Spectroscopy:

Periodic optical absorbance scans were conducted to monitor the formation of nanoparticles and confirm their stability. Absorbances were taken during the experiment in the UV range of 200-800 nm using SHIMADZU UV-1900 UV-Visible spectrophotometer.

2. Fourier Transform Infrared (FT-IR) Spectroscopy

The infrared spectra of samples were analysed by Bruker Vertex 80 Fourier Transform Infrared Spectrometer (Bruker alpha (10031705) with specifications of scan range 4000-650 cm-1; 32 scans and 8 cm-1 resolution). FTIR analysis was used to identify functional groups present in the *Macaranga peltata* leaf extract responsible for reducing ferric irons to iron nanoparticles (FeNPs), elucidating the interaction between the leaf extract phytochemicals and synthesized nanoparticles.

3. Powder X-ray Diffraction (XRD)

The crystalline nature and phase composition of the synthesized FeNPs were examined using Bruker D8 Focus X-ray Diffraction Spectrometer.

4. Scanning Electron Microscopy (SEM)

SEM analysis was carried out using Hitachi SU6600 Scanning Electron Microscope to analyze the surface morphology, size and distribution of the synthesized nanoparticles.

3 RESULTS & DISCUSSION

3.1 UV-Visible Spectroscopy Results

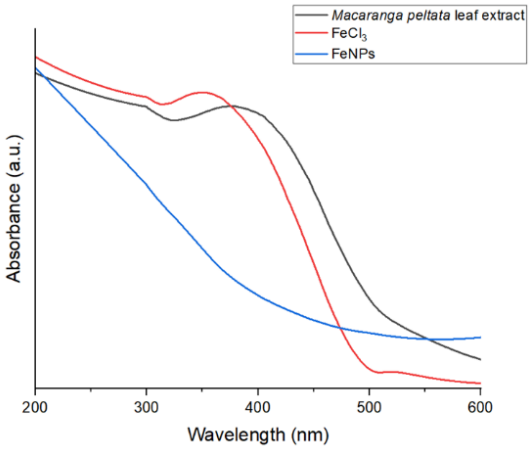

Figure 2. UV-Visible absorption spectra of a) *Macaranga peltata* leaf extract, b) $FeCl_3$ solution c) Synthesized FeNPs

Figure 2 illustrates the UV-vis spectra of a) $FeCl_3$, b) *Macaranga peltata* leaf extract and c) Fe nanoparticles in the 200-600 nm range. The formation of NPs was indicated by the color change of pale brown to blackish brown after the addition of the leaf extract to $FeCl_3$ solution. Leaf extract shows peaks at 280 and 450 nm while $FeCl_3$ shows a peak around 350 nm. The UV-vis spectra of the Fe NPs showed a continuous absorption from 200-600 nm. This well agrees with literature reported UV-vis spectra of amorphous Fe NPs.

3.2 FTIR Results

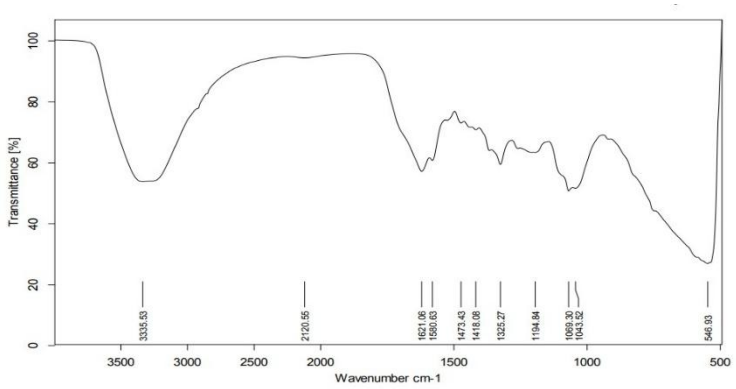

Figure 3. FTIR spectrum of Fe NPs synthesized using *Macaranga peltata* leaf extract

Figure 3 represents the FTIR spectrum of the prepared Fe NPs, indicating presence of organic compounds from *Macaranga peltata* leaf extract. This can be used to identify the functional groups of the phytochemicals responsible for reducing the metal precursor. It shows a prominent band at 3335 cm^{-1} due to intramolecular hydrogen bonded OH groups. In addition, the peaks at 1621 cm^{-1}, 1418 cm^{-}

[1], and 1100 cm^{-1} - 1030 cm^{-1} can be attributed to the C=O, in plane bending vibrations of O-H, and C-O-C stretching respectively.

3.3 XRD Results

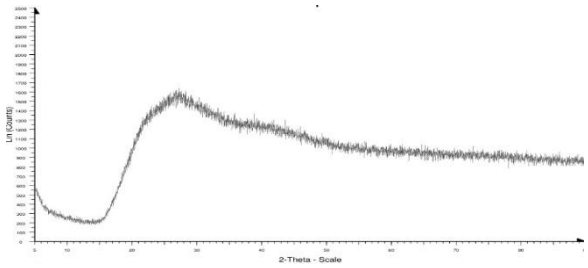

Figure 4. XRD pattern of Fe NPs synthesized using *Macaranga peltata* leaf extract

Figure 4 shows that the X-ray Diffraction of the synthesized iron nanoparticles using *Macaranga peltata* leaf extract. The pattern is deficient in distinct diffraction peaks, suggesting that the iron nanoparticles are amorphous in nature. The broad hump present at about $2\theta = 25^0$ is attributed to organic materials from *Macaranga peltata* leaf extract which can act as reducing and capping agents absorbed on the Fe NP surface.

3.4 SEM Results

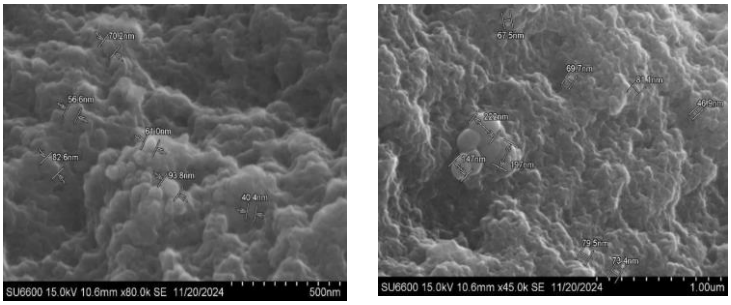

Figure 5. FE SEM Images of Fe NPs synthesized using *Macaranga peltata* leaf extract

The FE-SEM images of Fe NPs are shown in Figure 5. These images suggest that the particles agglomerate to form irregular clusters. This is due to the capping of Fe NPs with phytochemicals present in *Macaranga peltata* leaf extract. The diameter of these clusters' ranges from 34-94 nm.

3.5 Preparation of the Calibration Curve

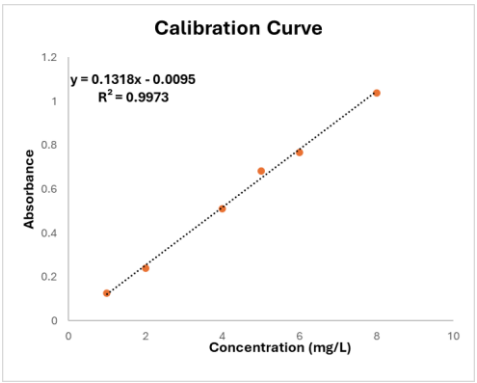

Figure 6. Calibration curve of methyl orange (concentration range: 1mg/L -8mg/L)

Figure 6 shows the calibration curve of methyl orange (MO), and the curve was prepared by taking known concentrations of 8,6,5,4,2,1 mg/L of MO as x-axis and absorbance at 464 nm as y-axis. The curve obeys Beers law in the studied concentration range. The linear regression of the calibration curve is y = 0.1318x - 0.0095; where y is absorbance and x is the concentration of MO (mg/L). The coefficient of correlation (R^2) of the regression analysis is 0.9973. The calibration curve was linear at the maximum wavelength and was therefore, suitable for estimating MO concentration.

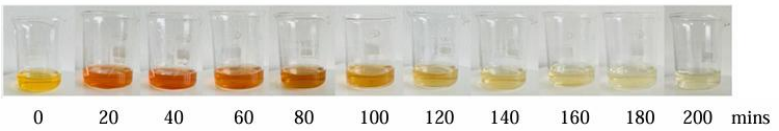

Figure 7. Degradation of MO in the presence of FeNPs

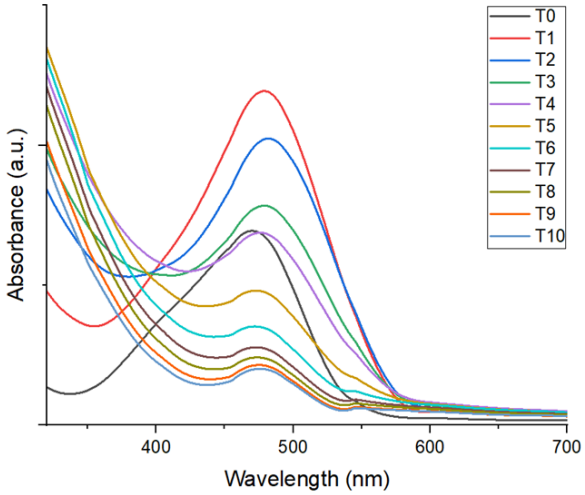

Figure 8. Kinetics of degradation of MO in the presence of the green catalyst-Fe NP (200-800 nm)

The degradation of MO using FeNPs and H_2O_2 was monitored using 2 mL withdrawing 2 mL samples from the mixture prepared in a previous step at time intervals of 20, 40, 60, 80, 100, 120, 140, 160, 180, 200 minutes and measuring absorbance over time. Figure 8 shows a gradual decrease in absorbance at 464 nm, indicating effective degradation. A significant reduction can be observed over 200 minutes, with final absorbance of 0.185, corresponding to a decrease in MO concentration and demonstrating the catalytic activity of FeNPs. The degradation process followed pseudo-first-order kinetics, with MO concentration diminishing consistently over time.

Figure 7 shows the visible fading of orange color, and the solution becomes significantly lighter by the end of 200 minutes, providing a qualitative representation of dye degradation process. The progressive color change visually supports the catalytic activity of FeNPs in enhancing dye degradation. In the initial stages of the reaction in Figure 7, a slight increase in absorbance was observed before the gradual decrease associated with dye degradation. This transient rise can be attributed to the formation of coloured intermediate species during the partial oxidation of methyl orange that absorb at the same or other wavelengths and/or increased light scattering from suspended catalyst particles and oxygen bubbles generated by the H2O2 decomposition. As the reaction progressed, these intermediates were further oxidized and turbidity reduced, leading to a steady decline in absorbance as the dye was removed .

MO decolorization was observed under the same conditions, using only H_2O_2 and without Fe NPs, to assess the capability of H_2O_2 alone to degrade the dye . No significant decolorization was observed for hydrogen peroxide alone (Figure 9).

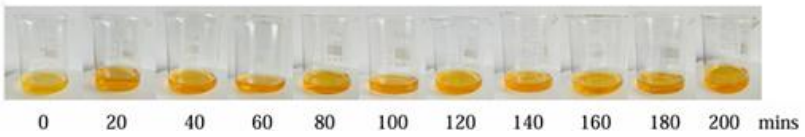

Figure 9. Degradation of MO in the absence of FeNPs

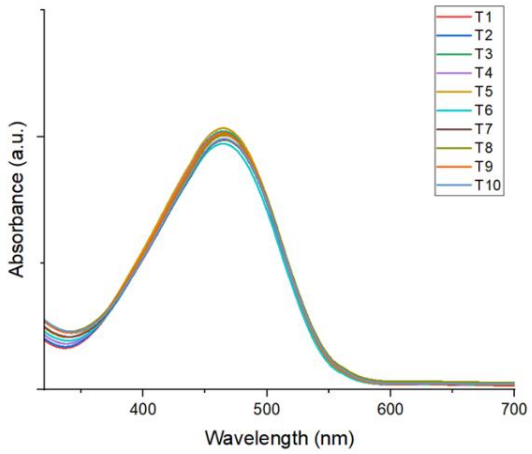

Figure 10. Kinetics of degradation of MO with just H_2O_2 and without Fe NPs (200-800 nm)

Figure 10 illustrates the variation of absorbance over different wavelengths during the control experiment using H_2O_2 without FeNPs. The absorbance remains relatively constant, fluctuating between 1.023 and 1.049 with minimal reduction over 200 minutes. Unlike the experiment with FeNPs, no notable reduction in the absorbance at the characteristic wavelength of 464 nm is evident. This indicates that, in the absence of FeNPs, H_2O_2 alone does not significantly contribute to MO degradation. Any observed changes in absorbances may be due to experimental noise or minor interactions between MO and H_2O_2. This graph does not exhibit exponential decay characteristic of pseudo-first-order kinetics. Figure 8 shows no visible change in orange color throughout the 0-200 minutes duration. The orange hue remains prominent, indicating that H_2O_2 alone is ineffective in degrading methyl orange.

Degradation of MO over time with Fe NP and MO with H_2O_2 only (without Fe NP)

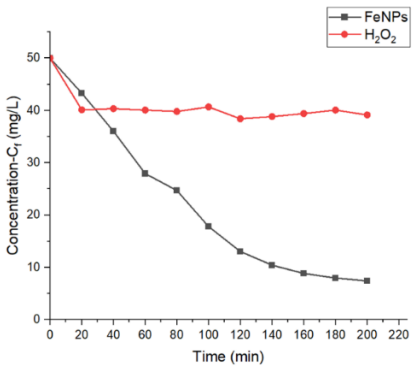

Figure 11.(a) Degradation of MO over time with Fe NPs + H_2O_2 b) Control- MO with H_2O_2 only (without Fe NPs)

In Figure 11, the "With FeNPs" curve shows a steep decline, visually representing the catalytic effect of FeNPs in breaking down MO.

Dye degradation Efficiency Evaluation in the presence of FeNPs

The initial and final concentration of MO can be determined using the calibration curve and the degradation efficiency (%) was 85.16 % in the presence of the Fe NPs. This indicates high efficiency of the Fe NPs in catalyzing MO degradation. Degradation efficiency of MO in the absence of Fe Nps remains relatively flat or slightly fluctuate, indicating the limited impact of H_2O_2 alone.

Dye degradation Efficiency Evaluation in the absence of FeNPs

The percentage degradation in the absence of FeNps was calculated to be 22.00 %. This low efficiency further confirms the ineffectiveness of H_2O_2 alone in degrading MO without the catalytic activity of Fe NPs. The combined graph (Figure 11) clearly illustrates the enhanced degradation kinetics when Fe NPs are present, validating their role as an effective green catalyst.

4 CONCLUSION

This work successfully demonstrated the green synthesis of FeNPs using *Macaranga peltata* leaf extract and assessed their catalytic efficiency in the degradation of methyl orange dye. The results proved that *Macaranga peltata* leaf bioactive compounds, mainly flavonoids and tannins, are effective both reducing and stabilizing agents for FeNPs. The green synthesized nanoparticles were amorphous in nature with sizes ranging from 34 to 94 nm, which are optimal for catalytic applications.

FeNPs synthesized in this work degraded 85.16% efficiency under optimized conditions within 200 minutes (3 hours and 20 minutes). Therefore, synthesized FeNPs may serve as a cost-effective environmentally friendly material for wastewater treatment. The study filled a critical research gap by exploring the underutilized *Macaranga peltata* for nanoparticle synthesis, linking sustainable nanotechnology with practical environmental applications. However, the following limitations such as single dye focus, concerns of reusability of nanoparticles and toxicity of by-products need to be addressed.

5 ACKNOWLEDGEMENTS

We would like to acknowledge the Sri Lanka Institute of Information Technology (SLIIT) for providing necessary resources for this research. Additionally, special thanks goes to Ms. Thavishi Chandratilake, for providing of lab resources and guidance on lab work, and to the Laboratory Manager, Mr.Sehan Jayasinghe from the Faculty of Humanities and Sciences at SLIIT, for providing access to lab resources. We also wish to express our great appreciation to the Sri Lanka Institute of Nanotechnology (SLINTEC) for offering analytical services for our samples.

REFERENCES

Abdeen, S., R.S, R. I., Geo, S., S, ornalekshmi, Rose, A., & P.K, P. (2013). Evaluation of Antimicrobial Activity of Biosynthesized Iron and Silver Nanoparticles Using the Fungi Fusarium Oxysporum and Actinomycetes SP. on Human Pathogens. *Nano Biomedicine and Engineering*, *5*(1). https://doi.org/10.5101/nbe.v5i1.p39-45

Ahmed, R. H., & Mustafa, D. E. (2019). Green synthesis of silver nanoparticles mediated by traditionally used medicinal plants in Sudan. *International Nano Letters*, *10*(1), 1–14. https://doi.org/10.1007/s40089-019-00291-9

Ashraf, M. A., Peng, W., Zare, Y., & Rhee, K. Y. (2018). Effects of Size and Aggregation/Agglomeration of Nanoparticles on the Interfacial/Interphase Properties and Tensile Strength of Polymer Nanocomposites. *Nanoscale Research Letters*, *13*(1). https://doi.org/10.1186/s11671-018-2624-0

Ebrahiminezhad, A., Taghizadeh, S., Ghasemi, Y., & Berenjian, A. (2018). Green synthesized nanoclusters of ultra-small zero valent iron nanoparticles as a novel dye removing material. *Science of the Total Environment*, *621*, 1527–1532. https://doi.org/10.1016/j.scitotenv.2017.10.076

ElHelaly, M. (2013). Nanotechnology, Occupational Health and Safety Concerns. *Journal of Postgenomics Drug & Biomarker Development*, *01*(03). https://doi.org/10.4172/2329-6879.1000116

Giun Tan, W., Ming Ng, W., Kang Lim, J., & Xin Che, H. (2018). Plantain Peel Mediated Green Synthesis Iron Oxide Nanoparticles, Surface Functionalization, and Them Performance towards Methylene Blue and Methyl Orange Dye Removal. *International Journal of Engineering & Technology*, *7*(3.36), 101. https://doi.org/10.14419/ijet.v7i3.36.29087

Iravani, S., & Zolfaghari, B. (2013). Green Synthesis of Silver Nanoparticles UsingPinus eldaricaBark Extract. *BioMed Research International*, *2013*, 1–5. https://doi.org/10.1155/2013/639725

Jiang, Z., Li, L., Huang, H., He, W., & Ming, W. (2022). Progress in Laser Ablation and Biological Synthesis Processes: "Top-Down" and "Bottom-Up" Approaches for the Green Synthesis of Au/Ag Nanoparticles. *International Journal of Molecular Sciences*, *23*(23), 14658. https://doi.org/10.3390/ijms232314658

Khoirotin, Nuhaa Faaizatunnisa, & Munasir Munasir. (2023). Green Synthesis of Fe3O4 Nanoparticles Using Green Betel Leaf Extract for Methylene Blue Adsorption. *Natural and Life Sciences Communications*, *22*. https://doi.org/10.12982/nlsc.2023.042

Megha M, Kavana D K, Rithin K, & Ramdas Bhat. (2024, October 20). *A Review On Phytochemistry And Pharmacology Of Macaranga Peltata» Article*. STM Journals. https://journals.stmjournals.com/article/article=2024/view=178897/

Raman, C. D., & Kanmani, S. (2018). Decolorization of Mono Azo Dye and Textile Wastewater using Nano Iron Particles. *Environmental Progress & Sustainable Energy*, *38*(s1), S366–S376. https://doi.org/10.1002/ep.13063

Ruan, W., Hu, J., Qi, J., Hou, Y., Zhou, C., & Wei, X. (2018a). Removal Of Dyes From Wastewater By Nanomaterials : A Review. *Advanced Materials Letters*, *10*(1), 9–20. https://doi.org/10.5185/amlett.2019.2148

Shahwan, T., Abu Sirriah, S., Nairat, M., Boyacı, E., Eroğlu, A. E., Scott, T. B., & Hallam, K. R. (2011). Green synthesis of iron nanoparticles and their application as a Fenton-like catalyst for the degradation of aqueous cationic and anionic dyes. *Chemical Engineering Journal*, *172*(1), 258–266. https://doi.org/10.1016/j.cej.2011.05.103

Wanakai, S. I., Kareru, P. G., Makhanu, D. S., Madivoli, E. S., Maina, E. G., & Nyabola, A. O. (2019). Catalytic degradation of methylene blue by iron nanoparticles synthesized using Galinsoga parviflora, Conyza bonariensis and Bidens pilosa leaf extracts. *SN Applied Sciences*, *1*(10). https://doi.org/10.1007/s42452-019-1203-z

Yusuf, M. (2019). Silver Nanoparticles: Synthesis and Applications. *Handbook of Ecomaterials*, 2343–2356. https://doi.org/10.1007/978-3-319-68255-6_16